Design and development of a 3RRS wearable fingertip cutaneous device

Francesco Chinello[1,2], Monica Malvezzi[1], Claudio Pacchierotti[1,2], and Domenico Prattichizzo[1,2]

***Abstract*— Wearable technologies are gaining great popularity in the recent years. The demand for devices that are lightweight and compact challenges researchers to pursue innovative solutions to make existing technologies more portable and wearable. In this paper we present a novel wearable cutaneous fingertip device with 3 degrees of freedom. It is composed of two parallel platforms: the upper body is fixed on the back of the finger, housing three small servo motors, and the mobile end-effector is in contact with the volar surface of the fingertip. The two platforms are connected by three articulated legs, actuated by the motors in order to move the mobile platform toward the user's fingertip and re-angle it to simulate contacts with arbitrarily oriented surfaces. Each leg is composed of two rigid links, connected to each other and then to the platforms, according to a RRS (Revolute-Revolute-Spherical) kinematic chain. With respect to other similar cable-driven devices presented in the literature, this device solves the indeterminacy due to the underactuation of the platform. This work presents the main design steps for the development of the wearable display, along with its kinematics, quasi-static modeling, and control. In particular, we analyzed the relationship between device performance and its main geometrical parameters. A perceptual experiment shows that the cutaneous device is able to effectively render different platform configurations.**

I. Introduction

Wearability of robotic devices will enable novel forms of human intention recognition through haptic signals and novel forms of communication and cooperation between humans and robots. Specifically, wearable haptics will enable devices to communicate with humans during their interaction with the environment they share [1]. Wearable haptic technology have been introduced in our everyday life by Sony. In 1997 its DualShock controller for PlayStation revolutionized the gaming industry by introducing a simple but effective vibrotactile feedback. By 2013, more than 400M units have been sold. In 2006, Nintendo released the game interface Wii Remote motion controller, which provides a similar feature, but wirelessly, and can be considered nowadays the most popular portable haptic interface, with over 100M sales. More recently, Apple unveiled the Apple Watch, which embeds a linear actuator that can make the watch vibrate. It is used whenever the wearer receives an alert or notification, or to communicate with other Apple Watch owners. You can get someone's attention with a gentle vibration, or even send some personal information like your heartbeat.

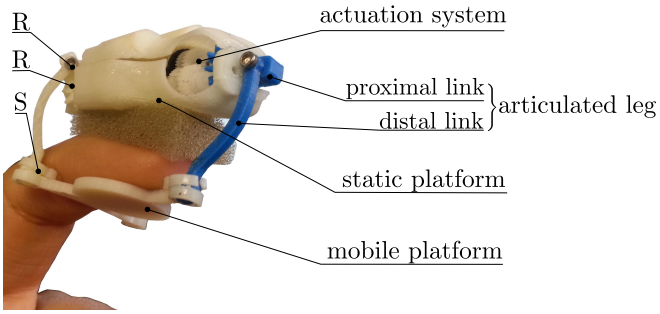

(a) Prototype

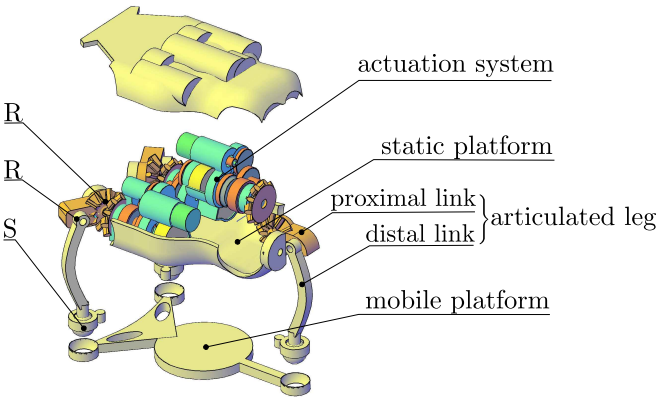

(b) CAD drawing

Fig. 1. The 3RRS wearable fingertip cutaneous device. The device is composed of two platforms. The static platform is fixed to the nail side of the finger and houses the actuators. The mobile platform is in contact with the fingertip and is in charge of applying the requested stimuli to the finger pad. The actuators move the platform by means of three articulated legs, constituting a 3RRS parallel mechanism.

However, the force feedback provided by these popular devices is still limited to vibrations, reducing the possibility of simulating any rich contact interaction. Towards a more realistic feeling of interacting with virtual and remote objects, researchers focused on glove-type haptic displays such as the Rutgers Master II and the CyberGrasp, which provide force sensations to all the fingers of the hand simultaneously. However, although they provide a compelling force feedback, these displays are still complex and *very* expensive. For this reason it becomes crucial to find a trade-off between a realistic feeling of touch and cost/wearability of the system. In this regard, we found *cutaneous technologies* very promising. Cutaneous tactile devices are haptic interfaces able to provide cutaneous haptic stimuli only. Cutaneous stimuli are detected by mechanoreceptors in the skin, enabling humans to recognize the local properties of objects such as shape,

The research leading to these results has received funding from the European Union Seventh Framework Programme FP7/2007-2013 under grant agreement n° 601165 of the project "WEARHAP - WEARable HAPtics for humans and robots" and from the Italian Ministry of Education, Universities and Research Futuro in Ricerca 2012 Programme with project "MODELACT" (Code RBFR12C608).

[1] Department of Information Engineering and Mathematics, University of Siena, Via Roma 56, 53100 Siena, Italy.

[2] Department of Advanced Robotics, Istituto Italiano di Tecnologia, Via Morego 30, 16163 Genova, Italy.

edges, and texture [2], [3]. Cutaneous feedback has been proved to play an important role in movement and weight perception [4], [5], [6], fine manipulation [7], precision grasping [8], and shape recognition [9]. Moreover, cutaneous feedback can provide an elegant way to simplify the design of haptic interfaces: the low activation thresholds and high fingertip densities of cutaneous receptors [4], [10] enable researchers to design cutaneous display devices that are small, lightweight, and inexpensive [1], [11].

An example of a cutaneous device exploiting these capabilities is the one presented by Minamizawa *et al.* [6], developed to display the weight of virtual objects. It consists of two motors that move a belt that is in contact with the user's fingertip. When the motors spin in opposite directions, the belt presses into the user's fingertip, while when the motors spin in the same direction, the belt applies a tangential force to the skin. This device was also used by Prattichizzo *et al.* [12] to display remote tactile experiences: an instrumented glove worn by a human sensed interaction forces at the remote environment, and the above cutaneous device presented those sensations to the user. Solazzi *et al.* [13] developed a three-degree-of-freedom (3-DoF) wearable cutaneous display to render virtual slanted surfaces. Four motors are placed on the forearm and two cables for each actuated finger are necessary to transmit the motor torque. More recently, Prattichizzo *et al.* [1] presented a wearable 3-DoF cutaneous device for interaction with virtual and remote environments. It consists of two platforms: one is located on the back of the finger, supporting three small DC motors, and the other is in contact with the volar surface of the fingertip. The motors shorten and lengthen three cables to move the platform toward the user's fingertip and re-angle it to simulate contacts with arbitrarily oriented surfaces. This device was used in [14] for immersive haptic interaction with virtual objects and in [15] to provide cutaneous feedback in a simulated robot-assisted surgery application. Three force-sensing resistors near the platform vertices measure the fingertip contact force for closed-loop control. Although quite effective, this device is underactuated, since it has three actuators to control the six-dimensional motion of the mobile platform interacting with the finger pad. The underactuation issue was there partially solved by introducing a simplified linear model of the fingertip compliance. However, the actual impedance properties of the fingertip are certainly more complex and cannot be captured by such a simple approach [16], [17], [18], [19].

An important issue affecting all the above mentioned devices is that their end-effectors *always* contact the fingerpad. They thus cannot provide the sensation of breaking and making contact with virtual and remote surfaces, cues that are known to be important to tactile interaction [20], [21]. Provancher *et al.* [22] designed the contact location display to overcome this limitation; it includes a roller that translates along as well as makes and breaks contact with the user's fingertip. Kuchenbecker *et al.* [23] employed a similar principle to create a non-actuated fingertip device that provides the user with the cutaneous sensation of making and breaking contact with virtual surfaces. When it is attached to a traditional haptic interface, force feedback deflects small internal springs and brings a shell into contact with the user's fingertip. More recently, Pacchierotti *et al.* in [24] presented a 3-DoF cutaneous device for remote tactile interaction. Its design is similar to the ones described in [1], but it adds three springs to enable the platform to make and break contact with the fingertip.

A. Contribution

In this paper we present a novel wearable haptic device for cutaneous stimulation, shown in Fig. 1. It is composed of two platforms: one is located on the back of the finger, supporting three small servo motors, and the other is in contact with the volar surface of the fingertip. The two platforms are connected by three articulated links, actuated by the motors so to be able to move the platform toward the user's fingertip and re-angle it to simulate contacts with arbitrarily oriented surfaces.

With respect to the cable-driven devices presented in [1], [24], this device solve the indeterminacy due to the underactuation of the platform. The platform of our proposed device, in fact, is moved through three articulated *legs*, constraining its motion in a three–dimensional subspace [25]. For this reason, we can present our device as a 3RRS (Revolute-Revolute-Spherical) parallel mechanism, with 3 degrees of freedom [26]. This mechanical structure decouples the position and force control problems and therefore simplify the control structure w.r.t. the solution proposed in [1]. Moreover, the overall control performance is increased, since we make no use of skin deformation models to determine the actuator inputs needed to apply a given force. Although they have served well, such models, in fact, do not guarantee accurate delivery of the desired force on the user's fingertip. Finally, as for [24], this device is able to make and break contact with the fingertip.

II. Device description

A prototype of the wearable cutaneous device is shown in Fig. 1a, while the CAD sketch is shown in Fig. 1b.

The mechanical structure of the device is parallel. It is composed of a static upper body and a mobile platform (end-effector), connected by three articulated legs that provide the required mobility. The device is worn by the user in such a way that the body and the motors are placed on the nail side of the finger, while the end-effector is placed in contact with the volar surface of the fingertip. This configuration enables the platform to move freely and reproduce surfaces with different orientations. The end-effector is connected to the body through three *legs*. Each leg is composed of two rigid links connected to each other and then with the body and the end-effector, according to a RRS (Revolute-Revolute-Spherical) kinematic chain. Three spherical (S) joints connect the distal links of the legs to the end-effector. One revolute (R) joint connect the distal and proximal links of each leg, and another revolute joint connect the proximal link of each leg to the body (see Fig. 1). The three revolute

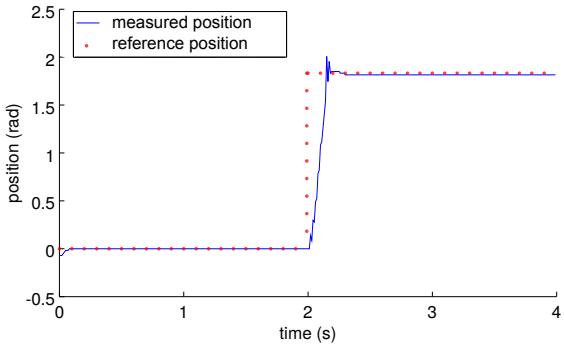

(a) Position control of a single actuator. The final position of the motor is set to 1.83 *rad*, and the rising time is 0.15 s.

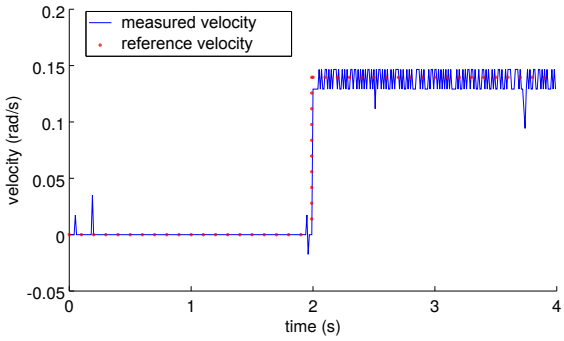

(b) Velocity control of a single actuator. The average error is 0.004 $\frac{rad}{s}$, and the reference speed is 0.14 $\frac{rad}{s}$.

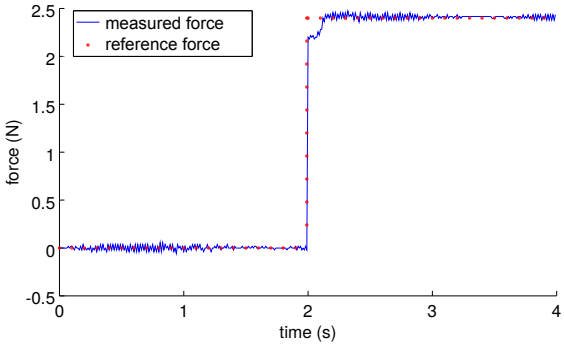

(c) Force control of a single actuator. The settling time is 0.2 s, the average error is 0.13 N, and the reference force is 2.4 N.

Fig. 2. Step response, velocity and force control performance of a single actuator. The settling times for the step response of the position, velocity, and force controls are 0.015 s, 0.14 s, and 0.2 s, respectively, while the average errors at the stationary phase are 0.02 rad, 0.23 rad/s, and 0.13 N, respectively.

joints between the proximal links and the body are actuated by the servo motors. In each leg, the axes of the two revolute joints are parallel, so that each leg constitute a 2-DoF articulated mechanism, constraining the motion of the center of each spherical joint on a plane fixed w.r.t. the body. The mobile platform has therefore 3-DoF w.r.t. the body. The motion of the mobile platform is analyzed in detail in Sec. III.

The actuators we used for our prototype are TGY-1370A sub micro servomotors. The housing of each actuator has been modified to minimize the size and weight of the device, as shown in Fig. 3, taking into account the geometric and

Control System	Atmega-328 μC
Operating Voltage range	4.8 to 6.0 V
Maximum Overall Normal Force	4.7 N
Updating Loop Time	30 ms
Roll Angle	$\pm\frac{\pi}{5}$
Pitch Angle	$\pm\frac{\pi}{6}$
Vertical Displacement	15 mm

TABLE I

FINGERTIP DEVICE FEATURES AND SPECIFICATIONS.

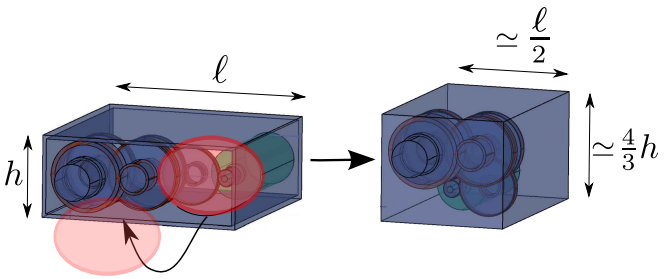

Fig. 3. Our customized servomotor. Folding the DC micromotor and the gearhead makes possible to reduce the width.

kinematic constraints of the mechanism. Each servomotor is composed of a 0510RN DC micromotor (Constar Micromotor Co., Ltd.), controlled by a KC2462 servo decoder (K&C Semitech Co., Ltd.). The servo decoder controls the position of the motor using the feedback of an analog potentiometer placed at the base of the output shaft. In order to be able to read the position of the potentiometer from an external AtMega328 microcontroller, a wire has been connected from the potentiometer to the analog input of the controller. Fig. 2a shows the step response of a single actuator with no load. While the position is controlled by the KC2462, the speed of the shaft is regulated by the external Atmega328 controller. The performance of the velocity control is shown in Fig. 2b. Finally, the performance of the force control for a single actuator is shown in Fig. 2c. To evaluate the exerted force, we connected a 15 mm link between the motor shaft and an ATI Mini 25 sensor (ATI Industrial Automation, Inc.).

The high stall torques provided by each servomotor allow us to reach a maximum force of 4.7 N on the platform. The overall performance and operative parameters of the device are summarized in Table I.

III. DEVICE ANALYSIS

A. Main definitions

The scheme of the wearable fingertip display is shown in Fig. 4. The device can be represented as a 3RRS parallel mechanism [26], [27].

Let us indicate with B_i, $i = 1,\ldots,3$ the centers of the spherical joint on the mobile platform and with O_1 the center of the circle passing through them, so that $\overline{B_iO_1} = b$. Let

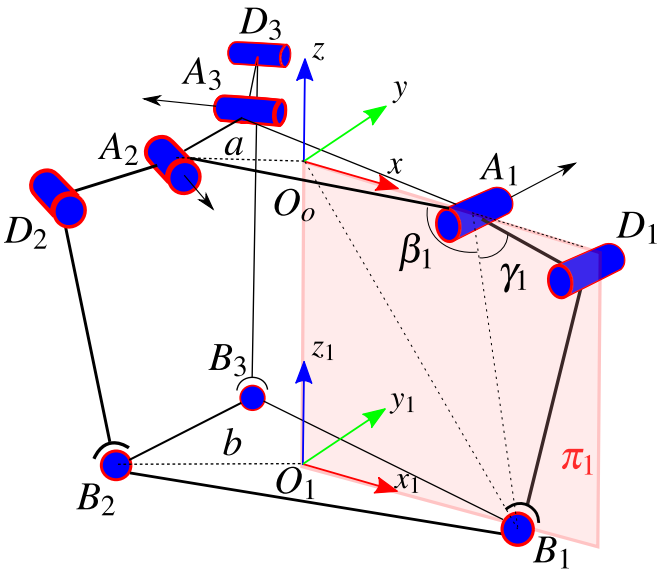

Fig. 4. Device kinematic scheme. The structure is characterized by a chain of two rotoidal joints followed by an spherical joint, one for each link. This configuration allows to the platform to perform roll along the x_1, pitch along y_1 and compression extension along z_1.

us indicate with $S_1 = \langle O_1, x_1, y_1, z_1 \rangle$ the reference frame in which the x_1 axis is parallel to $\overrightarrow{O_1 B_1}$, z_1 is orthogonal to the plane defined by the B_i points, and y_1 is consequently defined. Let us indicate with $b_i^1 = [b_{ix}^1, b_{iy}^1, b_{iz}^1]^{\mathrm{T}}$ the coordinates of each vertex B_i of the mobile platform, expressed in the S_1 reference frame.

Each leg is composed of two links: the first one is connected to the upper body trough a revolute joint, the second one is connected to the mobile platform through a spherical joint. The links are connected to each other through a revolute joint, whose axis is parallel to the one of the revolute joint fixed to the body. Let us indicate with u_i the unit vector identifying, for each leg, the direction of the revolute joint axes.

For each leg, we can then define the plane π_i passing through B_i and perpendicular to the revolute joint axes (in Fig. 4 part of π_1 is shown in pink). The axes intersect this plane in A_i and D_i. A_i correspond to the joints connecting each leg to the upper body, while D_i correspond to the middle joint. On the upper body we can then define point O_0 as the center of the circle passing through A_i, so that $\overline{A_i O_0} = a$. Let then $S_0 = \langle O_0, x, y, z \rangle$ be a reference frame on the upper body, with origin in O_0, x axis parallel to $\overrightarrow{O_0 A_1}$, z axis orthogonal to the plane defined by A_i, and y consequently defined. Let us indicate with $a_i = [a_{ix}, a_{iy}, a_{iz}]^{\mathrm{T}}$ the coordinates of A_i w.r.t. the S_0 frame.

The mobile platform will move w.r.t. the upper body according to the rotations imposed by the actuators to the joints passing through A_i and according to the kinematic constraints imposed by the mechanical structure. In particular, since the axes of the revolute joints of each leg are parallel, the motion they produce is plane. Moreover, we can observe that, for each leg $i = 1, \ldots, 3$, the B_i and D_i points move on the respective plane π_i, that passes through A_i and is perpendicular to u_i.

The coordinates of B_i w.r.t. S_0, $b_i = [b_{i,x}, b_{i,y}, b_{i,z}]^{\mathrm{T}}$, can be then evaluated as

$$b_i = p + R b_i^1, \tag{1}$$

where $p = [p_x, p_y, p_z]^{\mathrm{T}}$ contains the coordinates of O_1 w.r.t. S_0, and R is the rotation matrix between S_1 and S_0.

Since the B_i points move on three fixed planes π_i, the following constraint equations hold

$$b_{1,y} = 0, \quad \frac{b_{2,x}}{b_{2,y}} = c_2, \quad \frac{b_{3,x}}{b_{3,y}} = c_3, \tag{2}$$

where c_2 and c_3 are two constants that depends on the mechanism geometry. Eq. (2) introduces three constraints that limit the generic six-dimensional motion of the mobile platform. In particular, since three independent costraints have been introduced, the mobile platform will have three degrees of freedom.

The position and orientation of the mobile platform can be defined by the position of one point, namely O_1 w.r.t. S_0, described by its coordinates p, and by its orientation, described, for instance, through its Roll(ψ)–Pitch(θ)–Yaw(ϕ) angles $\varphi = [\psi, \theta, \phi]^{\mathrm{T}}$. Since the platform has 3 DoF, we can select three of these six variables and evaluate the remaining ones. In order to effectively render the orientation and stiffness of virtual and remote objects, a convenient choice for the *independent* variables includes the displacement in the z direction, p_z, and the roll (ψ) and pitch (θ) angles. Let us collect those variables in the vector $\xi = [p_z, \psi, \theta]^{\mathrm{T}}$. Recalling the rotation matrix expression as a function of RPY angles [28], and the constraints of eq. (2), we can evaluate the other variables, i.e., yaw angle ϕ, and p_x and p_y components of O_1 coordinates, as

$$\phi = \phi(p_z, \theta, \psi), \;\; p_x = p_x(p_z, \theta, \psi), \;\; p_y = p_y(p_z, \theta, \psi). \tag{3}$$

B. Inverse kinematics

In the inverse kinematics problem, the independent variables $\xi = [p_z, \psi, \theta]^{\mathrm{T}}$ are defined, and we want to evaluate the corresponding rotations $q = [q_1, q_2, q_3]^{\mathrm{T}}$ of the revolute joints in A_i. The objective is the definition of an inverse kinematics function $f_{ik} : \mathbb{R}^3 \to \mathbb{R}^3$ that allows to evaluate

$$q = f_{ik}(\xi). \tag{4}$$

For a given ξ, eq. (3) allows to complete the definition of vector p and rotation matrix R. Then, from eq. (1), it is possible to evaluate the coordinates of B_i w.r.t. S_0. Finally, the actuator rotation angles q_i can be evaluated as

$$q_i = \beta_i + \gamma_i, \tag{5}$$

where angles β_i and γ_i can be evaluated as follows

$$\beta_i = \arctan\left(\frac{s_{iz}}{\sqrt{s_{ix}^2 + s_{iy}^2}}\right), \;\; \gamma_i = \arccos\left(\frac{l_1^2 + s_i^2 - l_2^2}{2 l_1 |s_i|}\right), \tag{6}$$

where $s_i = b_i - a_i$, and l_1 and l_2 are the lengths of the proximal and distal link of each leg, respectively, i.e., $l_1 = |\overline{D_i A_i}|$, and $l_2 = |\overline{B_i D_i}|$.

C. Differential kinematics and statics

Let us indicate with v the velocity of O_1 and with ω the angular velocity of the mobile platform. The twist of the platform is then defined as $\nu = [v^{\mathrm{T}}, \omega^{\mathrm{T}}]^{\mathrm{T}}$. We can express the velocities of B_i, $i = 1, \ldots, 3$ as

$$v_{B_i} = v + \omega \times (b_i - p). \tag{7}$$

Since the B_i points move on planes perpendicular to the respective u_i directions, the following relationship holds

$$u_i^{\mathrm{T}} v - u_i^{\mathrm{T}} S(b_i - p)\omega = 0, \tag{8}$$

where the operator S, applied to a generic three dimensional vector, gives the corresponding skew matrix. Eq. (8) constitute three linear equations constraining the components of vectors v and ω, so that only three of the six components of ν are independent. Similarly to the position analysis described before, in our application we want to control the components v_z, ω_x (roll velocity) and ω_y (pitch velocity), collected in the vector $\dot{\xi} = [v_z, \omega_x, \omega_z]^{\mathrm{T}}$. From eq. (8) we can easily evaluate v_x, v_y and ω_z. We can then express the overall platform twist as

$$\nu = H\dot{\xi}, \tag{9}$$

where $H \in \mathbb{R}^{6\times 3}$ is a matrix whose components depend on platform configuration. The velocities of B_i can be also evaluated considering the articulated mechanism of each leg, as follow

$$v_{Bi} = \omega_i \times (d_i - a_i) + \omega_i' \times (b_i - d_i), \tag{10}$$

where $\omega_i = \dot{q}_i u_i$ are the angular velocities of the links connected to the upper body, actuated by the motors, and ω_i' are the angular velocities of the links connected to the mobile platform. The directions of both ω_i and ω_i' are parallel to u_i. From eq. (7) and (10), dot multiplying both sides by $(b_i - d_i)$, we get

$$(b_i - d_i)^{\mathrm{T}} v - (b_i - d_i)^{\mathrm{T}} S(b_i - p)\omega = (b_i - d_i)^{\mathrm{T}} S(d_i - a_i)\omega_i. \tag{11}$$

Collecting the actuator angular velocity magnitudes in a vector $\dot{q}$, eq. (11) can be written in a matrix form as

$$E\nu = F\dot{q}, \tag{12}$$

where $E \in \mathbb{R}^{3\times 6}$ and $F \in \mathbb{R}^{3\times 3}$ are matrices whose components depends on the coordinates of points A_i, B_i and D_i, In particular, F is a diagonal matrix. If F is invertible, from eq. (9), it is possible to evaluate the actuator velocities $\dot{q}$ as a function of the platform twist ν, i.e.,

$$\dot{q} = \tilde{J}\nu,$$

where $\tilde{J} = F^{-1}E \in \mathbb{R}^{3\times 6}$ is the *complete* Jacobian matrix. If we consider also the constraint in eq. (8), we can define the *constrained* Jacobian matrix $J = JH = F^{-1}EH \in \mathbb{R}^{3\times 3}$, relating the actuator angular velocities to the independent twist components, i.e.,

$$\dot{q} = J\dot{\xi}. \tag{13}$$

If the mechanism is not in a singular configuration, i.e., if J is full-rank, eq. (13) can be inverted to solve the direct differential kinematic problem $\dot{\xi} = J^{-1}\dot{q}$. The solution of this problem can be used to implement an iterative algorithm for the solution of the direct kinematic problem, i.e., to find $\xi = f_{dk}(q)$, where $f_{dk} : \mathbb{R}^3 \to \mathbb{R}^3$ is the inverse of the function f_{in} defined in eq. (4).

IV. Device Tests

In order to evaluate the performance of our wearable cutaneous device, we carried out a perceptual experiments aiming at evaluating the differential threshold on the inclination of the platform, in order to compare it with the literature on the neurophysiology of touch. The differential threshold can be defined as "the smallest amount of stimulus change necessary to achieve some criterion level of performance in a discrimination task" [29]. This gives us information about how different two platform configurations $\xi = [p_z, \psi, \theta]^{\mathrm{T}}$ should be in order to be perceived as different by the human user. This threshold is often referred to as just-noticeable difference or JND. Our hypothesis is that the JND of the orientation of the mobile platform is comparable to the one registered in the literature for human subjects interacting with real objects. The differential threshold of a perceptual stimulus reflects also the fact that people are usually more sensitive to changes in weak stimuli than they are to similar changes in stronger or more intense stimuli. The German physician Ernst Heinrich Weber proposed the simple proportional law $JND = kI$, suggesting that the differential threshold increases with increasing intensity I of the stimulus. Constant k is thus referred to as "Weber's fraction".

Six participants took part in the experiment, including two women and four men.

We evaluated the differential threshold for each controlled variable p_z, ψ, and θ using the simple up-down method [30]. We used a step-size of 1 mm, 1°, and 1°, for each variable p_z, ψ, and θ, respectively. We considered the task completed when six reversals occurred. Subjects were required to wear the cutaneous device on their right index finger as shown in Fig. 1a and tell the experimenter when the two stimuli provided felt different. We tested the JND at three standard stimuli: 10°, 15°, and 20° for ψ and θ, and 5 mm, 10 mm, and 15 mm for p_z. Each participant performed six trials of the simple up-down procedure, with two repetitions for each controlled variable. The average JND was calculated by finding individual JNDs and then averaging them together. Weber fractions for variables p_z, ψ, and θ resulted 0.13, 0.18, and 0.20, respectively, which is in agreement with previous results in the literature [31], [32].

V. Conclusion and Future Works

In this paper we presented a novel 3RRS wearable haptic display for cutaneous interaction, with 3 degrees of freedom. It is composed of two platforms: one located on the back of the finger, supporting three small servo motors, and the other in contact with the volar surface of the fingertip, in charge of applying the requested stimuli. The two platforms are

connected by three articulated links, actuated by the motors so to be able to move the platform toward the user's fingertip and re-angle it to simulate contacts with arbitrarily oriented surfaces. With respect to the cable-driven devices presented before in the literature, this device solves the indeterminacy due to the underactuation of the platform. We are currently integrating the device in a tactile rendering framework, i.e. a process by which desired sensory stimuli are imposed on the user in order to convey haptic cutaneous information about a virtual object. In the near future, we will carry out a more comprehensive experimental evaluation of the device's performance, both from the manipulability and perceptual points of view. The design and control of the device will be furthermore investigated. The mechanical model will be integrated with the statics and dynamics part, and sensitivity and optimization processes will be carried out, with the main objective of maximizing the performance, in terms of both mobility and wearability, of the device. Other types of parallel structures will be considered, to obtain different types of stimuli, e.g. translational or spherical mechanisms. In particular, in order to solve the direct kinematic problem, we will study and efficient way of implementing an iterative approach based on the Newton Raphson technique. This step is necessary for the implementation of a force control scheme.

REFERENCES

[1] D. Prattichizzo, F. Chinello, C. Pacchierotti, and M. Malvezzi, "Towards wearability in fingertip haptics: a 3-dof wearable device for cutaneous force feedback," *IEEE Transactions on Haptics*, vol. 6, no. 4, pp. 506–516, 2013.

[2] I. Birznieks, P. Jenmalm, A. W. Goodwin, and R. S. Johansson, "Encoding of direction of fingertip forces by human tactile afferents," *The Journal of Neuroscience*, vol. 21, no. 20, pp. 8222–8237, 2001.

[3] K. O. Johnson, "The roles and functions of cutaneous mechanoreceptors," *Current Opinion in Neurobiology*, vol. 11, no. 4, pp. 455–461, 2001.

[4] B. B. Edin and N. Johansson, "Skin strain patterns provide kinaesthetic information to the human central nervous system.," *The Journal of physiology*, vol. 487, no. Pt 1, pp. 243–251, 1995.

[5] C. Giachritsis, R. Wright, and A. Wing, "The contribution of proprioceptive and cutaneous cues in weight perception: early evidence for maximum-likelihood integration," in *Haptics: Generating and Perceiving Tangible Sensations*, pp. 11–16, 2010.

[6] K. Minamizawa, S. Fukamachi, H. Kajimoto, N. Kawakami, and S. Tachi, "Gravity grabber: wearable haptic display to present virtual mass sensation," in *Proc. of ACM Special Interest Group on Computer Graphics and Interactive Techniques*, pp. 8–es, 2007.

[7] R. Johansson and G. Westling, "Roles of glabrous skin receptors and sensorimotor memory in automatic control of precision grip when lifting rougher or more slippery objects," *Experimental brain research*, vol. 56, no. 3, pp. 550–564, 1984.

[8] G. Westling and R. Johansson, "Factors influencing the force control during precision grip," *Experimental Brain Research*, vol. 53, no. 2, pp. 277–284, 1984.

[9] J. Voisin, Y. Lamarre, and C. E. Chapman, "Haptic discrimination of object shape in humans: contribution of cutaneous and proprioceptive inputs," *Experimental Brain Research*, vol. 145, no. 2, pp. 251–260, 2002.

[10] R. S. Johansson and Å. B. Vallbo, "Tactile sensibility in the human hand: relative and absolute densities of four types of mechanoreceptive units in glabrous skin.," *The Journal of Physiology*, vol. 286, no. 1, pp. 283–300, 1979.

[11] C. Pacchierotti, A. Tirmizi, and D. Prattichizzo, "Improving transparency in teleoperation by means of cutaneous tactile force feedback," *ACM Transactions on Applied Perception*, vol. 11, no. 1, pp. 4–4, 2014.

[12] D. Prattichizzo, F. Chinello, C. Pacchierotti, and K. Minamizawa, "Remotouch: A system for remote touch experience," in *Proc. of IEEE International Symposium on Robots and Human Interactive Communications*, pp. 676–679, 2010.

[13] M. Solazzi, A. Frisoli, and M. Bergamasco, "Design of a cutaneous fingertip display for improving haptic exploration of virtual objects," in *Proc. of IEEE International Symposium on Robots and Human Interactive Communications*, pp. 1–6, 2010.

[14] L. Meli, S. Scheggi, C. Pacchierotti, and D. Prattichizzo, "Wearable haptics and hand tracking via an rgb-d camera for immersive tactile experiences," in *Proc. ACM Special Interest Group on Computer Graphics and Interactive Techniques Conference, SIGGRAPH*, 2014.

[15] L. Meli, C. Pacchierotti, and D. Prattichizzo, "Sensory subtraction in robot-assisted surgery: fingertip skin deformation feedback to ensure safety and improve transparency in bimanual haptic interaction," *IEEE Transactions on Biomedical Engineering*, vol. 61, no. 4, pp. 1318–1327, 2014.

[16] E. Serina, E. Mockensturm, C. Mote Jr, and D. Rempel, "A structural model of the forced compression of the fingertip pulp," *Journal of biomechanics*, vol. 31, no. 7, pp. 639–646, 1998.

[17] M. Srinivasan and K. Dankekar, "An investigation of the mechanics of tactile sense using two dimensional models of the primate fingertip," *Transactions of the ASME, Journal of Biomechanical Engineering*, vol. 118, pp. 48 – 55, 1996.

[18] J. Z. Wu, R. G. Dong, S. Rakheja, A. W. Schopper, and W. P. Smutz, "A structural fingertip model for simulating of the biomechanics of tactile sensation," *Medical Engineering and Physics*, vol. 26, no. 2, pp. 165 – 175, 2004.

[19] N. Nakazawa, R. Ikeura, and H. Inooka, "Characteristics of human fingertips in the shearing direction," *Biological Cybernetics*, vol. 82, pp. 207–214, 2000.

[20] B. B. Edin, L. Ascari, L. Beccai, S. Roccella, J.-J. Cabibihan, and M. Carrozza, "Bio-inspired sensorization of a biomechatronic robot hand for the grasp-and-lift task," *Brain research bulletin*, vol. 75, no. 6, pp. 785–795, 2008.

[21] G. Westling and R. S. Johansson, "Responses in glabrous skin mechanoreceptors during precision grip in humans," *Experimental Brain Research*, vol. 66, no. 1, pp. 128–140, 1987.

[22] W. R. Provancher, M. R. Cutkosky, K. J. Kuchenbecker, and G. Niemeyer, "Contact location display for haptic perception of curvature and object motion," *The International Journal of Robotics Research*, vol. 24, no. 9, pp. 691–702, 2005.

[23] K. Kuchenbecker, D. Ferguson, M. Kutzer, M. Moses, and A. Okamura, "The touch thimble: Providing fingertip contact feedback during point-force haptic interaction," in *Proc. of Symposium on Haptic interfaces for virtual environment and teleoperator systems*, pp. 239–246, 2008.

[24] C. Pacchierotti, F. Chinello, M. Malvezzi, L. Meli, and D. Prattichizzo, "Two finger grasping simulation with cutaneous and kinesthetic force feedback," in *Haptics: Perception, Devices, Mobility, and Communication*, pp. 373–382, 2012.

[25] J.-P. Merlet, *Parallel robots*, vol. 128. Springer Science & Business Media, 2006.

[26] J. Li, J. Wang, W. Chou, Y. Zhang, T. Wang, and Q. Zhang, "Inverse kinematics and dynamics of the 3-rrs parallel platform," in *Robotics and Automation, 2001. Proceedings 2001 ICRA. IEEE International Conference on*, vol. 3, pp. 2506–2511, 2001.

[27] L.-W. Tsai, *Robot analysis: the mechanics of serial and parallel manipulators*. John Wiley & Sons, 1999.

[28] L. Sciavicco and B. Siciliano, *Modelling and control of robot manipulators*. Springer Science & Business Media, 2000.

[29] G. A. Gescheider, *Psychophysics: the fundamentals*. Psychology Press, 2013.

[30] H. Levitt, "Transformed up-down methods in psychoacoustics," *The Journal of the Acoustical society of America*, vol. 49, no. 2B, pp. 467–477, 1971.

[31] W. R. Provancher, K. J. Kuchenbecker, G. Niemeyer, and M. R. Cutkosky, "Perception of curvature and object motion via contact location feedback," in *International Symposium on Robotics Research*, pp. 456–465, 2005.

[32] A. Bicchi, E. P. Scilingo, and D. De Rossi, "Haptic discrimination of softness in teleoperation: the role of the contact area spread rate," *IEEE Transactions on Robotics and Automation*, vol. 16, no. 5, pp. 496–504, 2000.